AN SCF POTENTIAL ENERGY SURFACE FOR LITHIUM CYANIDE

R. ESSERS, J. TENNYSON and P.E.S. WORMER
Institute of Theoretical Chemistry, University of Nijmegen, Toernooiveld, 6525 ED Nijmegen, The Netherlands

Received 14 April 1982

Ab initio SCF calculations are performed for LiCN using a large polarised GTO basis. An analytic fit to the two-dimensional surface (the CN bond length is frozen at 2.186 a_0) is presented.

1. Introduction

Recent microwave experiments [1] have shown that potassium cyanide has a triangular shape. This finding has been supported by ab initio SCF calculations [2–4]. The ab initio calculations predict that sodium cyanide is also triangular [3,4]. Lithium cyanide, on the other hand, is predicted to be linear and to have an isocyanide structure [5,6]. Numerous calculations [6–11] agree that hydrogen cyanide is linear with the H atom bound to the carbon atom, and this is born out by experiment [12].

These cyanides have in common that their bond to the metal atom is highly ionic, which is a consequence of the large electron affinity (experimental value: 3.82 eV [13]) of the cyanide and the low ionization potential of the alkali-metal atoms. Hence, the Coulomb force dominates the bonding, and as this force is isotropic the bending force constants of the alkali cyanides are exceptionally low. It is therefore interesting to study their rotational–vibrational spectra.

Computations, yielding these spectra, have been performed for LiCN [14] and for KCN [14–17]. The LiCN work was based on a rather crude potential, containing parameters fitted to the ab initio points of ref. [5]. Although many points of the surface of LiCN are given in ref. [5], it is difficult to extract a satisfactory analytic form from it [14]. So it seems worthwhile to perform a set of ab initio SCF calculations on LiCN, aiming especially at an accurate fit of the region of the potential energy surface of interest for the nuclear-motion calculations.

We conclude this paper by briefly addressing the question why the geometries of the alkali metal cyanides differ.

2. Calculations

All calculations have been performed with the ab initio SCF program ATMOL 3 [18]. No electron correlation has been considered. The gaussian (11s, 6p, 2d/6s, 3p, 2d) basis sets on carbon and nitrogen are the same as those used in earlier work [2]. An (11s, 4p/6s, 3p) basis was placed on the Li atom, with the s orbitals originating from van Duijneveldt's compilation [19]. The exponents of the p orbitals form the geometric sequence 0.025, 0.100, 0.400, 1.600 a_0^{-2}. The range covered by this sequence has been suggested by the work of Williams and Streitweiser [20]. The two most compact p orbitals are contracted with the coefficients appearing in the first virtual p orbital of the Li^+ ion; the two diffuse p orbitals have been left uncontracted. The energy of the lithium atom in this basis is 8×10^{-5} au above the Hartree–Fock limit [21], the calculated ionization potential is 5.341 eV (experimental value is 5.390 eV [22]), its computed polarizability is 144.0 a_0^3 (expt.: 148 a_0^3 [23]), and the polarizability of the Li^+ ion in this basis is 0.1875 a_0^3 (expt.: 0.193 a_0^3 [24]). In total we performed 43 separate SCF calculations. The geometries were located on four circles of radii 3.3, 3.8, 4.3 and 4.8 a_0. Each circle consisted of ten points dictated by the

0 009-2614/82/0000–0000/$ 02.75

Gauss–Legendre integration scheme, as explained below. The last three points were chosen on a circle of radius 2.8, for angles where the repulsive exchange effects were still comparatively small.

In all calculations the CN bond distance has been kept fixed at $2.186\,a_0$, the optimum Hartree–Fock distance of the CN^- anion [2].

A simple argument, based on Coulomb's law, the computed electron affinity of the CN radical (3.25 eV [2]), and the ionization potential of the lithium atom, predicts that the transfer of one electronic charge from the atom to the diatom becomes energetically favourable at a distance of $13\,a_0$. Analysis of the dipole moment at a distance of $4.8\,a_0$ between the lithium atom and the center of mass of the cyanide confirms that indeed the transfer of one electron has taken place. At this distance, and in a triangular structure, 84.7% of the SCF dipole moment arises from the separation of charge; 14.4% of the dipole moment is caused by the polarization of the CN^- anion; polarisation of the Li^+ ion accounts for 0.1%. We attribute the remaining 0.8% to exchange and penetration effects. The latter effects account for 11.2% of the dipole moment at a distance of $3.8\,a_0$. So, it is clear that to a very good approximation LiCN may be thought to consist of two closed-shell ions.

The SCF interaction energy between two closed-shell monomers consists of two parts: a short-range energy, due to exchange and penetration, and a damped long-range energy. The long-range energy is the same as the electrostatic and induction energy appearing in classical electrostatic theory. Dispersion forces are not accounted for by the independent-particle model.

The (classical) electrostatic energy is given by the expression [2]

$$E_{\mathrm{cl}}(R,\theta)=\sum_{L=0}^{\infty} R^{-L-1}P_L(\cos\theta)\langle Q_{L0}^{\mathrm{A}}\rangle. \tag{1}$$

Here is R the length of $\boldsymbol{R}$, a vector pointing from the center of nuclear mass of $^{12}C-^{14}N$ towards the Li nucleus; θ is the angle of $\boldsymbol{R}$ with $\boldsymbol{r}$, a vector pointing from nitrogen to carbon. The function $P_L(\cos\theta)$ is a Legendre polynomial of order L [25], and $\langle Q_{L0}^{\mathrm{A}}\rangle$ is the (expectation value of the) Lth order multipole moment of the CN^- ion. In the derivation of eq. (1) the fact has been used that Li^+ possesses only one permanent moment (its charge).

The (classical) induction energy can be written similarly,

$$E_{\mathrm{ind}}(R,\theta)=\sum_{l_1,l_2=0}^{\infty} R^{-l_1-l_2-2} \times \sum_{L=|l_1-l_2|}^{l_1+l_2} P_L(\cos\theta)\,C_{l_1 l_2 L}. \tag{2}$$

A formula for the induction coefficients $C_{l_1 l_2 L}$ in terms of the polarizability tensors of the monomers has been given in ref. [2]. The short-range energy is expressed as

$$E_{\mathrm{SR}}(R,\theta)=\sum_{L=0}^{\infty} D_L(R)\,P_L(\cos\theta), \tag{3}$$

where

$$D_L(R)=\tfrac{1}{2}(2L+1)\int_{-\pi}^{0} E_{\mathrm{SR}}(R,\theta)\,P_L(\cos\theta)\,\mathrm{d}(\cos\theta). \tag{4}$$

Because Legendre polynomials are complete and orthogonal eqs. (3) and (4) are in principle exact expressions.

The total interaction energy is represented by

$$E_{\mathrm{tot}}(R,\theta)=[E_{\mathrm{cl}}(R,\theta)+E_{\mathrm{ind}}(R,\theta)]\,F(R) + E_{\mathrm{SR}}(R,\theta), \tag{5}$$

where $F(R)$ is an isotropic damping function. After some experimentation with different analytic forms we took the gaussian form

$$F(R)=1-\exp[-a(R-R_0)^2]. \tag{6}$$

Expression (5) for the total energy contains a number of parameters to be fitted to the ab initio SCF energy. To this end we have used the following procedure. The permanent moments of the cyanide up to and including $L=6$ were taken from ref. [2], where the same basis for the cyanide had been used. Also the induction coefficients, modified for the Li^+ ion, were taken from ref. [2]. We then guessed initial values for the damping parameters a and R_0 defined in eq. (6). Having fixed the long-range energy in this manner, we simply computed the short-range energy E_{SR} as the difference of the long-range and the SCF interaction energy. This short-range energy was then substituted into the

integral, appearing in eq. (4), and the integral was evaluated by a ten-point Gauss–Legendre quadrature, yielding ten parameters $D_L, L = 0, \ldots, 9$, for a fixed value of R. These short-range parameters were finally represented by the analytic form

$$D_L(R) = \exp[-A_L - B_L R - C_L R^2]. \quad (7)$$

In order to obtain the 30-fit parameters A_L, B_L and C_L we have calculated $D_L(R)$ by the present procedure for $R = 3.3, 3.8, 4.3$ and $4.8\ a_0$ and applied a least-squares polynomial fit to $\ln(D_L)$. After finding a fit to the short-range energy in this manner, we redetermined the damping parameters a and R_0 by a least-squares fit of the total energy (5) to the 43 available SCF points, with a and R_0 as the free variables. The whole procedure was repeated until the values for the 32-fit parameters a, R_0, A_L, B_L and C_L ($L = 0, \ldots, 9$) did not change any further.

3. Results and discussion

The electrostatic and induction coefficients defined by eqs. (1) and (2) are given in table 1 for L from 0 to 6. This table differs in two places from the one given in ref. [2]: here C_{111} contains the polarizability of the Li^+ ion, and not of the K^+ ion, and C_{211} is derived from a finite field (coupled Hartree–Fock) polarizability, whereas before an uncoupled value was presented. Optimum values for the parameters appearing in the damping function (6) are $a = 1.5156\ a_0^{-2}$ and $R_0 = 1.9008\ a_0$. The final short-range parameters A_L, B_L and C_L, defined by eq. (7) are listed in table 2.

The fit of the SCF energy surface is excellent: the mean deviation of the fitted values from the 43 computed values is 0.22% and the largest deviation is 0.99%. However, the full physical potential energy surface is not covered by it. Beyond $R \approx 13\ a_0$, where the charge transfer of an electron from lithium to the cyanide takes place, the closed-shell SCF model breaks down, as it cannot describe the proper dissociation into neutral species. This also implies that the long-range energy, as given by eqs. (1) and (2), loses its meaning and has to be replaced for $R \gtrsim 13.0\ a_0$ by dispersion energy expressions. Also the fitting parameters impose constraints on the applicability of the fitted surface. For small R the value of the damping parameter R_0 ($= 1.9008\ a_0$) forms a limitation. For large R it is the appearance of parameters C_L with negative sign which gives a restriction. With positive B_L this implies that the fitted value of $D_L(R)$ as a function of R goes through a minimum and then goes to infinity for large R. The nearest of such minima occurs for D_6 at $R = 9.34\ a_0$. However, the short-range energy is here less than 0.2% of the long-range energy and so the repulsive terms can safely be neglected in this region.

Table 2
Short-range parameters of LiCN (in au) [cf. eqs. (7) and (8)]

L	A_L	B_L	C_L
0	−1.38321	0.14001	0.207892
1	−2.95791	1.47977	−0.011613
2	−4.74203	1.81199	−0.017818
3	−1.88853	1.28750	0.027728
4	−4.41433	2.32297	−0.070693
5	−4.02565	2.77538	−0.137720
6	−5.84259	3.48085	−0.186311
7	−2.61681	2.65559	−0.005882
8	−6.34466	4.34498	−0.152914
9	15.2023	−6.54925	1.302568

Table 1
Long-range coefficients [a] (in au) between Li^+ and CN^- [cf. eqs. (1) and (2)]

	$L = 0$	$L = 1$	$L = 2$	$L = 3$	$L = 4$	$L = 5$	$L = 6$
$\langle Q_{L0} \rangle$	−1.00	−0.2151	−3.414	−3.819	−15.84	−14.29	−43.82
C_{11L}	−10.53		−3.17				
C_{21L}		−10 31		2 03			
C_{22L}	−57.49		−35.71		5.23		
C_{31L}			−35.56		5.95		
C_{32L}		−101.45		−37.62		−14.23	
C_{33L}	−458.2		−353.7		−112.6		−108.3

[a] Expressed with respect to a coordinate system with the origin in the center of mass of $^{12}C-^{14}N$.

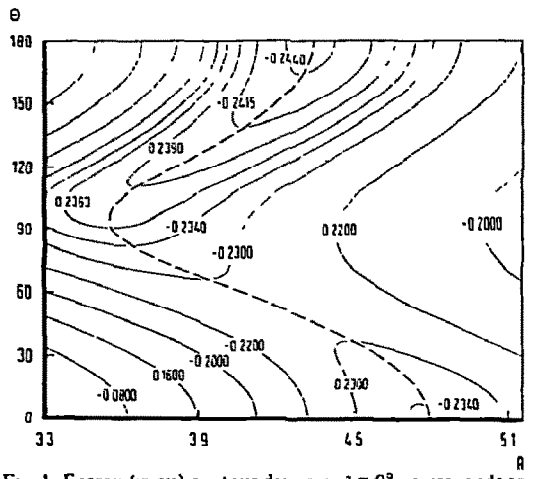

Fig. 1. Energy (in au) contour diagram. $\theta = 0°$ corresponds to LiCN; $\theta = 180°$ corresponds to LiNC. Dashed line is the path of minimum energy.

The fit of the surface is very suitable for the calculation of nuclear bound states. Work in this direction is in progress.

In fig. 1 a contour diagram is presented for the region of the potential energy surface of interest for rotational–vibrational calculations. The path of minimum energy is shown as a dashed line. In fig. 2 this same

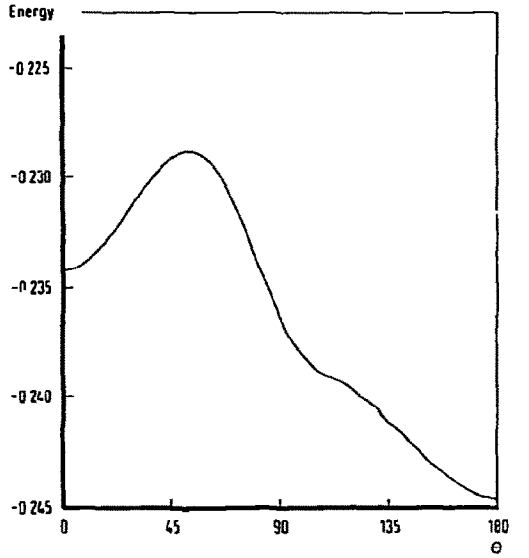

Fig 2. Energy (in au) variation along path of minimum energy, the dashed line in fig. 1. $\theta = 0°$ corresponds to LiCN, $\theta = 180°$ to LiNC.

path, which in fact is the reaction path for the isomerization of LiCN, is plotted. The shoulder at $\theta = 100°$ corresponds to the sharp bend of the dashed line at $R = 3.6\,a_0$ in fig. 1. The height of the barrier in fig. 2 is 3.42 kcal/mol above the cyanide ($\theta = 0°$) energy. The isomerization energy is 6.49 kcal/mol, in good agreement with the value 6.21 kcal/mol found by Clementi et al. [5] with the use of a large STO basis and for optimized CN bond lengths. Inclusion of correlation brings the isomerization energy down to 3.9 kcal/mol [6]. Clementi et al. [5] also considered nonlinear LiCN, and used for that purpose a large GTO basis which is very similar to ours. The main difference is that we have two polarization functions on the carbon and the nitrogen atom and Clementi et al. one. It is therefore surprising that they report not to have found a barrier for isomerization. A possible explanation for this disagreement is that their grid was too coarse, so that the barrier was overlooked. If that is not the case one is forced to conclude that the barrier height is extremely basis-set dependent.

The path of minimum energy is given as a polar graph in fig. 3, where one sees that the path is elliptic, but not as symmetric as the corresponding path in KCN. Some properties of LiCN and LiNC at optimum R are given in table 3.

We conclude this paper by saying a few words about the geometries of the alkali cyanides. It is argued in section 2 that the bond in LiCN, just as in KCN [2], is ionic and that the interaction energy separates into a short- and a long-range component. These components are shown in fig. 4 as a function of the angle θ at the distance $R = 4.350\,a_0$ (the optimum R of

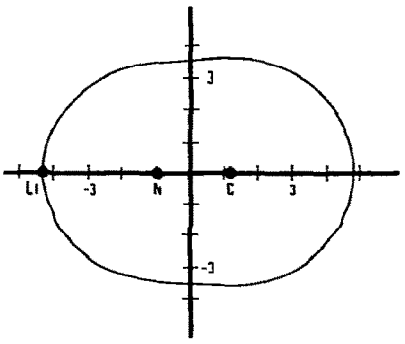

Fig. 3. R values (in au) of minimum energy as a function of θ plotted in a polar graph. The equilibrium structure of LiNC is shown.

Table 3
Some properties of equilibrium LiCN and LiNC (in au). Molecule along z axis, origin in the center of mass of $^{12}C-^{14}N$

	LiCN	LiNC
z coordinate Li	4.795	−4.350
z coordinate C	1.00892	1.00892
z coordinate N	−1.17708	−1.17708
energy	−99.809126	−99.819166
dipole moment	3.7415	−3.5081
quadrupole moment [a]	18.336	14.634
octopole moment [b]	102.7	−83.13
field gradient at N [c]	1.2671	0.7411
field gradient at Li [c]	0.0472	0.0469

[a] $(3z^2 - r^2)/2$. [b] $(5z^3 - 3zr^2)/2$. [c] $-(3z^2 - r^2)/r^5$.

the isocyanide structure). The long-range energy (dashed line) as well as the short-range energy (full line) show a behaviour which is qualitatively the same as in KCN (cf. fig. 2 of ref. [2]). In KCN the final position of the alkali atom is mainly determined by the short-range (exchange) repulsion. It is likely that this is true too for NaCN, which is also triangular [3,4]. However, in LiCN the most stable geometry is determined by a subtle balance: the short-range repulsion favours a triangular structure, the long-range energy prefers the cyanide structure and the final isocyanide structure is a compromise. The ionic model applied to HCN predicts a linear cyanide structure, because of the absence of exchange repulsion in the interaction of the proton with the cyanide. So, the exchange interaction is the predominant factor determining the structure of the electron-rich alkali cyanides, the long-range attraction determines the structure of HCN, and LiCN shows a compromise.

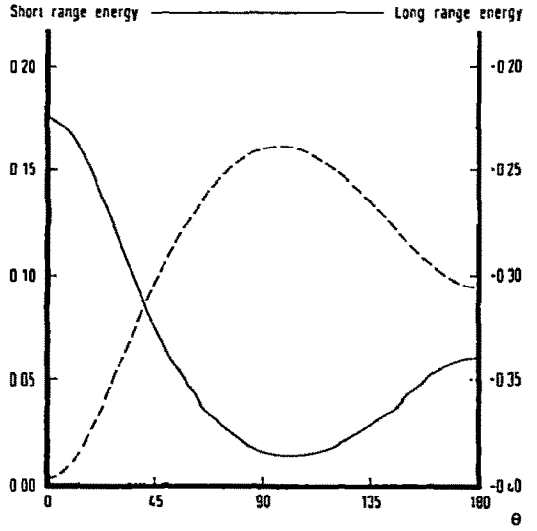

Fig 4. Long-range energy (dashed line) and short-range energy (full line) as a function of θ. $R = 4.350\,a_0$. $\theta = 0°$ corresponds to LiCN, $\theta = 180°$ to LiNC.

References

[1] T. Törring, J.P. Bekooy, W.L. Meerts, J. Hoeft, E. Tiemann and A. Dymanus, J. Chem. Phys. 73 (1980) 4875.
[2] P.E.S. Wormer and J. Tennyson, J. Chem. Phys. 75 (1981) 1245.
[3] M.L. Klein, J.D. Goddard and D.G. Bounds, J. Chem. Phys. 75 (1981) 3909.
[4] C.J. Marsden, J. Chem. Phys., to be published.
[5] E. Clementi, H. Kistenmacher and H. Popkie, J. Chem. Phys. 58 (1973) 2460.
[6] L.T. Redmon, G.D. Purvis and R.J. Bartlett, J. Chem. Phys 72 (1980) 986.
[7] P.K. Pearson, H.F. Schaefer III and W. Wahlgren, J Chem. Phys. 62 (1975) 350.
[8] U. Wahlgren, J. Pacansky and P.S. Bagus, J. Chem. Phys. 63 (1975) 2874.
[9] J.E. Gready, G.B. Bacskay and N.S. Hush, Chem. Phys. 31 (1978) 467.
[10] J. Pacansky, N.S. Dalal and P.S. Bagus, Chem. Phys. 32 (1978) 183.
[11] C.E. Dykstra and D. Secrest, J. Chem. Phys. 75 (1981) 3967.
[12] A.G. Maki and R.L. Sams, J. Chem. Phys. 75 (1981) 4178.
[13] J. Berkowitz, W.A. Chupka and T.A. Walter, J. Chem. Phys. 50 (1969) 1497.
[14] V.A. Istomin, N.F. Stepanov and B.I. Zhilinskii, J. Mol. Spectry. 67 (1977) 265.
[15] J. Tennyson and B.T. Sutcliffe, Mol. Phys., to be published.
[16] J. Tennyson and A. van der Avoird, J. Chem. Phys., to be published.
[17] J. Tennyson and B.T. Sutcliffe, to be published.
[18] V.R. Saunders and M.F. Guest, Daresbury Research Laboratory, Warrington, UK.
[19] F.B. van Duijneveldt, IBM Report RJ 945 (1971).
[20] J.E. Williams and A. Streitwieser, Chem. Phys. Letters 25 (1974) 507.
[21] E. Clementi, IBM J. Res. Develop. Suppl. 9 (1965) 2.
[22] R.C. Weast, ed., Handbook of chemistry and physics, 58th Ed. (Chemical Rubber Company, Cleveland, 1977).
[23] G.E. Chamberlain and J.C. Zorn, Phys. Rev. 129 (1963) 677.
[24] J.R. Tessman, A.H. Kahn and W. Shockley, Phys. Rev. 92 (1953) 890.
[25] A.R. Edmonds, Angular momentum in quantum mechanics, 2nd Ed. (Princeton Univ. Press, Princeton, 1960).